



March 2004

# Out-of-plane mosaic of single-wall carbon nanotube films

Wei Zhou

*University of Pennsylvania*

Karen I. Winey

*University of Pennsylvania*, winey@lrsm.upenn.edu

John E. Fischer

*University of Pennsylvania*, fischer@seas.upenn.edu

T. V. Sreekumar

*Georgia Institute of Technology*

S. Kumar

*Georgia Institute of Technology*

*See next page for additional authors*

Follow this and additional works at: [http://repository.upenn.edu/mse\\_papers](http://repository.upenn.edu/mse_papers)

## Recommended Citation

Zhou, W., Winey, K. I., Fischer, J. E., Sreekumar, T. V., Kumar, S., & Kataura, H. (2004). Out-of-plane mosaic of single-wall carbon nanotube films. Retrieved from [http://repository.upenn.edu/mse\\_papers/121](http://repository.upenn.edu/mse_papers/121)

Reprinted from *Applied Physics Letters*, Volume 84, Issue 12, March 2004, pages 2172-2174. Publisher URL: <http://dx.doi.org/10.1063/1.1689405>

This paper is posted at Scholarly Commons. [http://repository.upenn.edu/mse\\_papers/121](http://repository.upenn.edu/mse_papers/121)

For more information, please contact [libraryrepository@pobox.upenn.edu](mailto:libraryrepository@pobox.upenn.edu).

---

# Out-of-plane mosaic of single-wall carbon nanotube films

## **Abstract**

For single-wall carbon nanotube (SWNT) films deposited from suspension onto filter membranes, or by drop casting or spin coating onto flat substrates, the tube axes lie preferentially in the film plane. Using x-ray scattering and a two-dimensional detector, we show that this out-of-plane mosaic spread can be easily and accurately quantified. It varies significantly with deposition conditions, and the aligning effects of deposition and external force in the film plane (e.g., magnetic field) are additive. Films from well-dispersed tubes show better alignment than from poor dispersions. The finite out-of-plane mosaic in C<sub>60</sub>@SWNT films enables quantitative separation of one-dimensional diffraction (chains of C<sub>60</sub> peas) from the 2D rope lattice diffraction.

## **Comments**

Reprinted from *Applied Physics Letters*, Volume 84, Issue 12, March 2004, pages 2172-2174. Publisher URL: <http://dx.doi.org/10.1063/1.1689405>

## **Author(s)**

Wei Zhou, Karen I. Winey, John E. Fischer, T. V. Sreekumar, S. Kumar, and H. Kataura

## Out-of-plane mosaic of single-wall carbon nanotube films

W. Zhou, K. I. Winey, and J. E. Fischer<sup>a)</sup>

*Department of Materials Science and Engineering and Laboratory for Research on the Structure of Matter, University of Pennsylvania, Philadelphia, Pennsylvania 19104*

T. V. Sreekumar and S. Kumar

*School of Polymer, Textile and Fiber Engineering, Georgia Institute of Technology, Atlanta, Georgia 30332*

H. Kataura

*Department of Physics, Tokyo Metropolitan University, Tokyo 192-0397, Japan*

(Received 11 November 2003; accepted 27 January 2004)

For single-wall carbon nanotube (SWNT) films deposited from suspension onto filter membranes, or by drop casting or spin coating onto flat substrates, the tube axes lie preferentially in the film plane. Using x-ray scattering and a two-dimensional detector, we show that this out-of-plane mosaic spread can be easily and accurately quantified. It varies significantly with deposition conditions, and the aligning effects of deposition and external force in the film plane (e.g., magnetic field) are additive. Films from well-dispersed tubes show better alignment than from poor dispersions. The finite out-of-plane mosaic in  $C_{60}$ @SWNT films enables quantitative separation of one-dimensional diffraction (chains of  $C_{60}$  peas) from the 2D rope lattice diffraction. © 2004 American Institute of Physics. [DOI: 10.1063/1.1689405]

In order to maintain the excellent axial properties expected from perfect single-wall carbon nanotubes (SWNT),<sup>1</sup> various methods<sup>2–6</sup> have been developed to obtain macroscopically oriented materials. In Fig. 1(a), we show schematically partially aligned SWNT fiber and films. We showed that SWNT alignment in fibers (axially symmetric about  $z$ )<sup>7</sup> and the in-plane ( $xy$ ) preferred orientation of free-standing SWNT films<sup>8</sup> can be obtained by combining two-dimensional (2D) x-ray fiber diagrams with polarized Raman scattering. The out-of-plane ( $xz$ ) alignment has received much less attention.<sup>9</sup> Here we report an easy method to measure the out-of-plane mosaic.

The traditional approach to this problem is the x-ray or neutron “rocking curve.” Using a point detector and a geometry with incident, detected, and diffracted wave vectors  $\mathbf{K}_i$ ,  $\mathbf{K}_f$ , and  $\mathbf{Q} = \mathbf{K}_f - \mathbf{K}_i$  all coplanar, the sample angle  $\theta$  is scanned symmetrically about  $2\theta_B/2$ , where  $\theta_B$  is fixed at a convenient Bragg angle. The normal to the film plane is either perpendicular (for out-of-plane mosaic) or parallel (for in-plane mosaic) to  $\mathbf{K}_i$ . For semicrystalline nanotube ropes the first peak occurs near  $2\theta = 6^\circ$  with Cu x rays. This is generally less than the mosaic full-width at half maximum (FWHM), so accurate corrections for the sampled volume and absorption are necessary.<sup>9</sup> Neglecting these corrections leads to erroneously small FWHM’s.<sup>10</sup>

Measurements using 2D area detectors are much easier. Sampling geometries are essentially the same while anisotropic scattering intensities originating from the one-dimensional (1D) character of SWNT and the 2D rope lattice are recorded directly without any correction for sampled volume. Also the FWHM is less sensitive to the generally smaller absorption corrections. The SWNT mosaic can be obtained from  $\chi$ -dependent intensity integrated over appro-

priate radial ( $\mathbf{Q}$ ) sectors; the azimuthal angle  $\chi$  is equivalent to the rocking curve  $\theta$ .

X-ray fiber diagrams were measured<sup>11</sup> on film samples consisting of several strips  $\sim 0.5$  mm wide and  $\sim 10$  mm long, stacked parallel to each other in 0.7 mm capillaries. To obtain the out-of-plane mosaic, the film plane was parallel to the incident beam as illustrated in Fig. 1(b).<sup>12</sup> We studied eight films prepared by different methods. One was deposited from suspension in a 26-T magnetic field, resulting in partial in-plane alignment along the  $H$  axis.<sup>6</sup> We expect this film to exhibit an out-of-plane mosaic narrower than the in-plane value due to the additional driving force associated with the filter deposition geometry. Conversely, films deposited with no field will have some out-of-plane alignment but random in-plane orientation. The effect of dispersion was studied by comparing films deposited from SWNT/H<sub>2</sub>O/NaDDBS (sodium dodecylbenzene sulfonate),<sup>13</sup> and from SWNT/methanol. Films deposited on smooth substrates from SWNT/oleum<sup>14</sup> and SWNT/H<sub>2</sub>O were also compared. Uniaxial high pressure applied to nanotube soot yields pellets with out-of-plane alignment.<sup>9</sup> We prepared a 0.5-mm-thick pellet by pressing purified SWNT powder at 700 atm.

Figure 2(a) is the detector image from a 26-T-aligned film. The out-of-plane mosaic was obtained by summing pixels in  $2.4^\circ$  radial sectors  $1^\circ$  wide in  $\chi$ , centered at  $2\theta = 6.3^\circ$  [the (1 0) Bragg position]. The result is plotted in Fig. 2(b), where the solid curve is the fit to a Gaussian centered at  $\chi = 180^\circ$  plus a constant.<sup>15</sup> The Gaussian FWHM is  $\sim 27^\circ$ , significantly smaller than the in-plane FWHM ( $\sim 34^\circ$ ).<sup>8</sup>

We summarize the thicknesses, densities, and mosaics of the eight films in Table I. The  $H$ -aligned film has the best out-of-plane alignment because the magnetic force aligns the tubes both in-plane and out-of-plane. The films from H<sub>2</sub>O/NaDDBS suspensions have smaller out-of-plane mosaics ( $44^\circ$ – $49^\circ$ ) than the one from methanol suspension ( $77^\circ$ ), while the film deposited from oleum ( $44^\circ$ ) is better than the one from H<sub>2</sub>O without surfactant ( $62^\circ$ ). SWNT in

<sup>a)</sup>Electronic mail: fischer@lrsm.upenn.edu

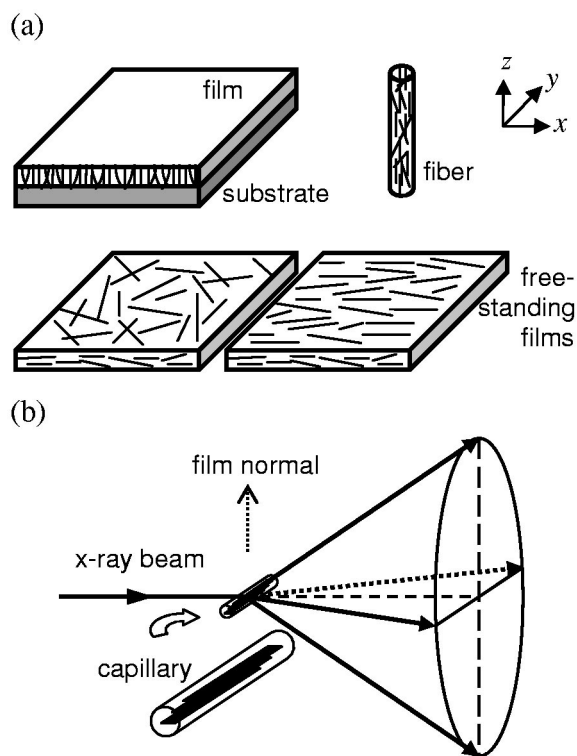


FIG. 1. (a) Schematic of various macroscopically oriented SWNT materials. Tubes in a fiber are preferentially aligned along the fiber axis ( $z$  axis). For films, the tube axes may either orient preferentially normal to the film plane (e.g., aligned nanotube arrays grown on a substrate by chemical vapor deposition method) or lie preferentially in the film plane (e.g., films deposited from suspension onto filter membranes, or by drop casting or spin coating onto flat substrates). The first case is analogue to the fiber in terms of alignment since all tubes are preferentially oriented along the  $z$  axis. The second type of film is often free standing, with nanotubes preferentially oriented parallel to the film plane ( $xy$  plane) while within the film plane, tubes can be either randomly oriented (e.g., ordinary buckypaper) or partially aligned (e.g., with a magnetic field). In this case, preferred orientations are the  $xy$  plane and the  $x$  axis for films without and with in-plane alignment respectively. (b) Schematic of the experimental setup for measuring out-of-plane mosaic. The film plane is parallel to the incident x-ray beam. Out-of-plane alignment results in azimuth( $\chi$ )-dependent anisotropic scattering within the 2D detector plane.

$H_2O$  with added NaDDBS contains mainly isolated nanotubes,<sup>13</sup> and oleum is also a good dispersant.<sup>14</sup> On the contrary, stable SWNT suspensions cannot be obtained in methanol or  $H_2O$  without surfactant. Large SWNT aggregates remaining in poor dispersions will limit the out-of-plane alignment. Films 12, 17, and 29  $\mu\text{m}$  thick from  $H_2O/\text{NaDDBS}$  all have similar FWHMs, whereas a thickness dependence was observed in  $H$ -aligned films.<sup>8</sup> Finally, the pellet shows little out-of-plane alignment, FWHM  $\sim 98^\circ$ . This is not unexpected since dry SWNT powders consist mainly of randomly oriented and entangled SWNT aggregates. High pressure may dramatically decrease the volume of macroscopic pores resulting in high density, but is unable to untangle SWNT aggregates and introduce significant alignment. Based on the above analysis, we expect the best out-of-plane alignment and also the highest density to be achieved by gentle deposition from well-dispersed SWNT suspension with the aid of outside forces such as magnetic, electrical, or shear fields.

$C_{60}$ @SWNT (peapod) films<sup>16</sup> have no in-plane preferred orientation. Using the geometry of Fig. 1(b), the nonzero

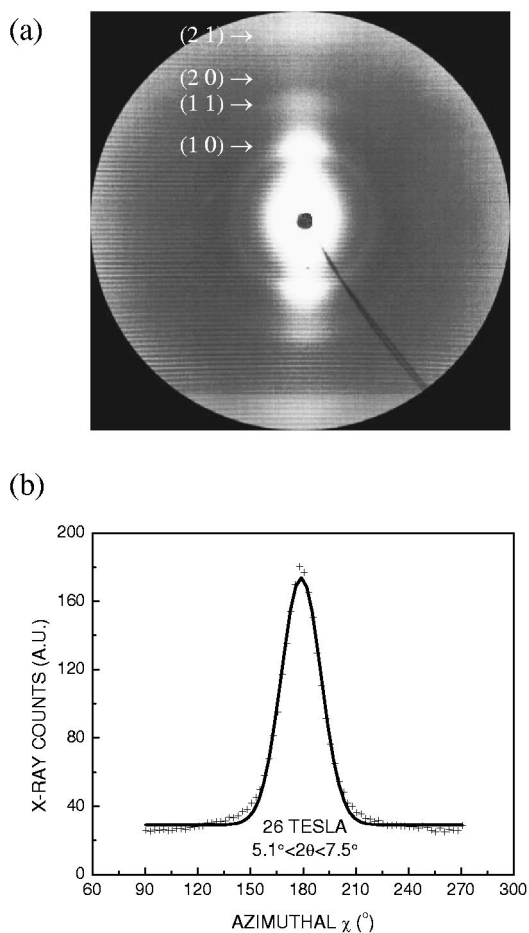


FIG. 2. (a) Detector image from a 26-T-aligned SWNT film measured with its plane parallel to the incident x-ray beam. Anisotropic intensities directly reflect the out-of-plane alignment. (b) Background-subtracted x-ray counts, summed over intervals  $5.1^\circ < 2\theta < 7.5^\circ$  about the (1,0) 2D rope lattice reflection, every  $1^\circ$  in  $\chi$ . Data are the symbols; fit to a Gaussian plus a constant is the smooth curve. The deduced out-of-plane FWHM is  $\sim 27^\circ$ , significantly smaller than the in-plane mosaic ( $34^\circ$ ) due to the additional effect of the deposition of long 1D objects on a flat surface.

out-of-plane mosaic allows us to detect both the 1D (pea) and 2D (pod) lattices simultaneously, and for the first time to separate these in a bulk sample using x-ray diffraction. In Fig. 3(a) we show the detector image. Diffraction peaks from the 1D peas and 2D pods are concentrated along the horizontal and vertical axes respectively, similar to selected area electron diffraction from a single peapod rope.<sup>17</sup> No ( $hkl$ ) diffraction was observed indicating the absence of chain-chain correlations.

Azimuthal integrations of the 2D data  $10^\circ$  wide in  $\chi$  centered at  $90^\circ$ ,  $135^\circ$ , and  $180^\circ$  give the equivalent of wide-angle x-ray profiles with different fractional 1D and 2D components. Knowing the out-of-plane mosaic ( $59^\circ$ ), we can quantitatively separate the 1D and 2D behavior. In Fig. 3(b) we show the pea (II) and pod (III) profiles. Previously reported x-ray results from randomly oriented peapods are superpositions of both.<sup>16</sup> We also show the profile of the control sample (I). The intensity of the (1, 0) rope peak is substantially reduced after filling with buckyballs due to cancellation of amplitudes from pea and pod. This is used to calculate the filling fraction of SWNTs by  $C_{60}$  in this film,  $\sim 80\%$ . From profile III, the first-order 1D diffraction peak

TABLE I. Summary of the thicknesses, densities, out-of-plane, and in-plane mosaics for eight films produced under various conditions.  $\text{FWHM}_{\text{out}}$  and  $\text{FWHM}_{\text{in}}$  are the out-of-plane and in-plane Gaussian distribution widths of SWNT axes with respect to the film plane and in-plane preferred axis respectively. The values listed represent the samples we measured; any of these parameters could vary with other factors such as deposition rate, SWNT concentration, thickness, membrane material, etc.

Method	Filter deposition			Direct deposition		Uniaxial press
	SWNT/H <sub>2</sub> O with Triton X-100	SWNT/H <sub>2</sub> O with NaDDBS	SWNT /Methanol	SWNT /oleum	SWNT /H <sub>2</sub> O	SWNT powder
External field	26 T magnetic	...	...	...	...	...
Thickness ( $\mu\text{m}$ ) ( $\pm 5\%$ )	7	12	17	20	14	18
Density ( $\text{g}/\text{cm}^3$ ) ( $\pm 5\%$ )	0.9	0.5	0.5	0.4	0.7	0.5
$\text{FWHM}_{\text{out}}$ (deg)	27°	46°	49°	44°	77°	44°
$\text{FWHM}_{\text{in}}$ (deg)	34°	...	...	...	...	...

has a sawtooth line shape. The mean  $C_{60}$  separation is  $9.68 \text{ \AA}$  by fitting the peak to a broadened Gaussian modulated by a sawtooth function. This value agrees well with high resolution transmission electron microscope lattice images of isolated peapods ( $9.68 \text{ \AA}$ ),<sup>17</sup> and is slightly smaller than the value calculated from the peak position ( $9.77 \text{ \AA}$ ).<sup>16</sup> It is surprising that the 1D chains have a mean lattice constant significantly smaller than that of the 3D fcc crystal; if anything, the lower coordination would argue for larger peapod separation.

Clearly the pod environment is playing an important role.<sup>18</sup>

This work was supported by ONR Grant N00014-01-1-0657. Central facility support was provided by the NSF MRSEC Program, Grant DMR00-79909. H.K. thanks the Grant-in-Aid for Scientific Research (A) No. 13304026 from the Ministry of Education, Culture, Sports, Science, and Technology of Japan.

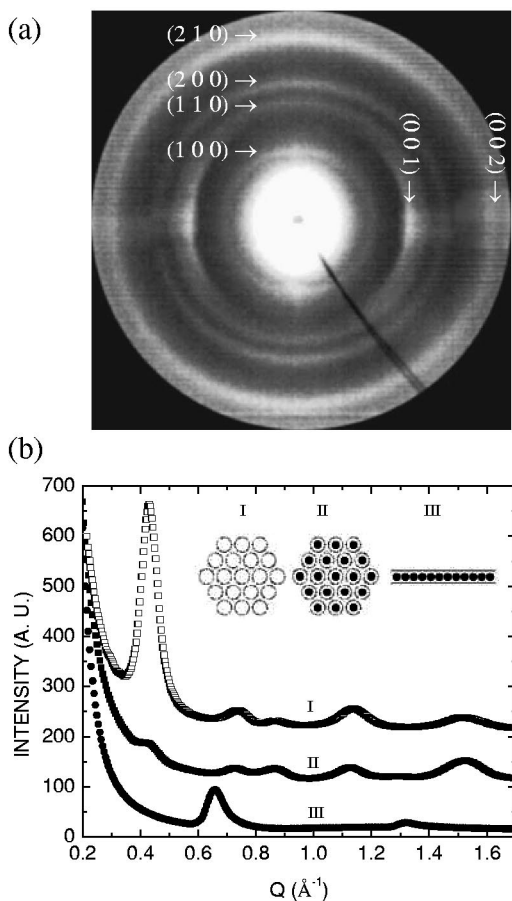


FIG. 3. (a) Detector image from a  $C_{60}$ @SWNT peapod film. Diffraction peaks from the 1D  $C_{60}$  lattice are concentrated in the direction perpendicular to those from the 2D pod lattice, a consequence of the out-of-plane partial alignment. (b) X-ray diffraction patterns from the starting SWNT film (control sample), and  $C_{60}$ @SWNT film (peapod sample). Note the filling of  $C_{60}$  into nanotubes significantly changes the diffraction profile. The (001) and (002) peaks from the  $C_{60}$  chains are easily detected.

<sup>1</sup>R. Saito, G. Dresselhaus, and M. S. Dresselhaus, *Physical Properties of Carbon Nanotubes* (Imperial College Press, London, 1998).

<sup>2</sup>L. Jin, C. Bower, and O. Zhou, *Appl. Phys. Lett.* **73**, 1197 (1998).

<sup>3</sup>R. Haggenueller, H. H. Gommans, A. G. Rinzler, J. E. Fischer, and K. I. Winey, *Chem. Phys. Lett.* **330**, 219 (2000).

<sup>4</sup>B. Vigolo, A. Penicaud, C. Coulon, C. Sauder, R. Pallier, C. Journet, P. Bernier, and P. Poulin, *Science* **290**, 1331 (2000).

<sup>5</sup>D. A. Walters, M. J. Casavant, X. C. Qin, C. B. Huffman, P. J. Boul, L. M. Ericson, E. H. Haroz, M. J. O'Connell, K. Smith, D. T. Colbert, and R. E. Smalley, *Chem. Phys. Lett.* **338**, 14 (2001).

<sup>6</sup>P. Launois, A. Marucci, B. Vigolo, A. Derre, and P. Poulin, *J. Nanosci. Nanotechnol.* **1**, 125 (2001).

<sup>7</sup>W. Zhou, J. Vavro, C. Guthy, K. I. Winey, J. E. Fischer, L. M. Ericson, S. Ramesh, R. Saini, V. A. Davis, C. Kittrell, M. Pasquali, R. H. Hauge, and R. E. Smalley, *J. Appl. Phys.* **95**, 649 (2004).

<sup>8</sup>J. E. Fischer, W. Zhou, J. Vavro, M. C. Llaguno, C. Guthy, R. Haggenueller, M. J. Casavant, D. E. Walters, and R. E. Smalley, *J. Appl. Phys.* **93**, 2157 (2003).

<sup>9</sup>N. Bendiab, R. Almairac, J.-L. Sauvajol, S. Rols, and E. Elkaim, *J. Appl. Phys.* **93**, 1769 (2003).

<sup>10</sup>B. Q. Wei, R. Vajtai, Y. Y. Choi, P. M. Ajayan, H. Zhu, C. Xu, and D. Wu, *Nano Lett.* **2**, 1105 (2002).

<sup>11</sup><http://www.lrsm.upenn.edu/lrsm/facMAXS.html> (description of apparatus).

<sup>12</sup>The film plane was ensured to be parallel to the incident beam with the aid of an x-ray imaging camera. Scattered intensity was corrected for absorption by the sample, and background scattering from the empty capillary, etc., was subtracted. The  $\chi$  resolution is better than  $2.6^\circ$  (measurement of graphite with known FWHM). The real out-of-plane FWHMs could be  $0^\circ$ – $5^\circ$  smaller than the measured values due to misalignment of several sandwiched films.

<sup>13</sup>M. F. Islam, E. Rojas, D. M. Bergey, A. T. Johnson, and A. G. Yodh, *Nano Lett.* **3**, 269 (2003).

<sup>14</sup>T. V. Sreekumar, T. Liu, S. Kumar, L. M. Ericson, R. H. Hauge, and R. E. Smalley, *Chem. Mater.* **15**, 175 (2003).

<sup>15</sup>A better fit was achieved by adding a Lorentzian component while the area-weighted average FWHM ( $26^\circ$ ) is quite close to the value obtained with just the Gaussian, so we use pure Gaussian for comparison purposes.

<sup>16</sup>H. Kataura, Y. Maniwa, M. Abe, A. Fujiwara, T. Kodama, K. Kikuchi, H. Imahori, Y. Misaki, S. Suzuki, and Y. Achiba, *Appl. Phys. A: Mater. Sci. Process.* **74**, 349 (2002).

<sup>17</sup>B. W. Smith, R. M. Russo, S. B. Chikkannanavar, and D. E. Luzzi, *J. Appl. Phys.* **91**, 9333 (2002).

<sup>18</sup>M. Hodak, Ph.D. thesis, University of Pennsylvania, 2002, in which can be found an as yet unpublished LDA calculation which gives the experimental lattice constant to within  $0.01 \text{ \AA}$ .